ELSEVIER

Remote Sensing of Environment 76 (2001) 130–137

Remote Sensing of Environment

www.elsevier.com/locate/rse

Parameterization of vegetation backscatter in radar-based, soil moisture estimation

Rajat Bindlish[a], Ana P. Barros[b,*]

[a]SSAI, USDA/ARS Hydrology Laboratory, Beltsville, MD, USA

[b]Division of Engineering and Applied Sciences, Harvard University, 118 Pierce Hall, 29 Oxford Street, Cambridge, MA 02138, USA

Received 22 May 2000; accepted 28 October 2000

Abstract

The Integral Equation Model (IEM) was previously used in conjunction with an inversion model to retrieve soil moisture using multifrequency and multipolarization data from Spaceborne Imaging Radar C-band (SIR-C) and X-band Synthetic Aperture Radar (X-SAR). Convergence rates well above 90%, and small RMS errors were attained, for both vegetated and bare soil areas, using radar data collected during Washita 1994. However, the IEM was originally developed to describe the scattering from bare soil surfaces only, and, therefore, vegetation backscatter effects are not explicitly incorporated in the model. In this study, the problem is addressed by introducing a simple, semiempirical, vegetation scattering parameterization to the multifrequency, soil moisture inversion algorithm. The parameterization was formulated in the framework of the water–cloud model and relies on the concept of a land-cover (land-use)-based dimensionless vegetation correlation length to represent the spatial variability of vegetation across the landscape and radar-shadow effects (vegetation layovers). An application of the modified inversion model to the Washita 1994 data lead to a decrease of 32% in the RMSE, while the correlation coefficient between ground-based and SAR-derived soil moisture estimates improved from 0.84 to 0.95.

Keywords: Vegetation; Backscatter; Soil moisture; Radar; Inverse methods; Retrieval

1. Introduction

Previously, Bindlish and Barros (2000) used the Integral Equation Model (IEM) developed by Fung, Li, and Chen (1992) in conjunction with an inversion algorithm to retrieve soil moisture using multifrequency and multipolarization data from Spaceborne Imaging Radar C-band (SIR-C) and X-band Synthetic Aperture Radar (X-SAR). The RMS error in the estimated soil moisture was of the order of 0.05 cm^3/cm^3 for data collected during the Washita 1994 experiment (Starks & Humes, 1996), which is comparable to the effect of noise in the SAR data.

The original IEM model was, however, developed for bare soil conditions only, and although the retrieval algorithm performed well even for vegetated areas (convergence rates were well above 90%), a valid concern is whether it would be equally successful when dense vegetation is present. Vegetation canopies complicate the retrieval of moisture in the underlying soil, because the canopies contain moisture of their own. Thus, the retrieved surface water content corresponds to the combined signatures of vegetation and soil water. Due to multiple scattering effects, the interaction between the two contributions and the observed backscatter is highly nonlinear. The key research question is, therefore, how to separate the contribution of vegetation backscatter and absorption from that of soil moisture.

Use of remote sensing techniques in the optical domain (visible and shortwave infrared) to monitor vegetation canopies over space and time has been well-documented in the literature (Asrar, Kanemasu, Jackson, & Pinter, 1985; Sellers, 1985; Tucker, Vanpraet, Sharman, & Van Ittersum, 1985). Cloud cover, however, strongly limits the number of available optical images. In addition, these techniques are limited by the observed saturation of the observed signal with increasing biomass.

Radar provides a useful tool for assessing biomass, since it is unaffected by cloud cover or low solar zenith angles

* Corresponding author. Tel.: +1-617-495-2858; fax: +1-617-496-1457.

E-mail address: barros@deas.harvard.edu (A.P. Barros).

0034-4257/00/$ – see front matter
PII: S0034-4257(00)00200-5

(a potentially significant problem at high latitudes). The backscatter from vegetation canopies is determined by many factors including: (1) the dielectric constant of the vegetation material, which is strongly influenced by moisture content; (2) the size distribution of the scatters in a canopy; (3) the shape distribution of the scatterers in a canopy; (4) the orientation distribution of the scatterers in a canopy; (5) the canopy cover's geometry (row direction and spacing, cover fraction, etc.); and (6) the roughness and dielectric constant of the underlying soil surface. At higher viewing angles, the backscattering contribution of the canopy increases and is dominated by the return from vertically aligned stalks and cobs where they exist, whereas the canopy loss component is dominated by the leaves (Ulaby, Moore, & Fung, 1986).

In the context of radar applications, backscatter at high frequencies (C- and X-bands) will be dominated by scattering processes in the crown layer of branches and foliage in the canopy, whereas backscatter at lower frequencies (P- and L-bands) is dominated by scattering processes involving major woody biomass components (trunks and branches) (Imhoff, 1995; McDonald, Dobson, & Ulaby, 1991; Ulaby, Sarabandi, McDonald, Whitt, & Dobson, 1990). Cimino, Casey, Rabassa, and Wall (1986) and Wu (1987) demonstrated that SAR data can be used to discriminate different forest types, and that the intensity in a SAR image at L-band is proportional to the aboveground biomass of the forest stands.

For soil moisture retrieval, the sensitivity of the radar backscatter signal is significantly higher at lower frequencies (Fung, 1994; Ulaby et al., 1986), whereas at higher frequencies, the signal is more sensitive to vegetation (Prevot et al., 1993; Ulaby et al., 1986). A combination of high- and low-frequency SAR data was used by Prevot et al. (1993) and Taconet et al. (1994) to improve the estimation of soil moisture. These studies suggested that the vegetation scattering for low-frequency SAR data was important only when vegetation density was high. Moreover, in humid environments, the soil moisture is also high, and so is its contribution to the observed backscatter. The contribution of vegetation in the scattering process is significantly smaller than that of soil in areas of sparse vegetation, and in principle, the vegetation scattering can be neglected. In arid and semiarid regions, however, soil moisture content rarely exceeds 20%, and, thus, the soil contribution may be small or approximately the same in magnitude as the vegetation contribution.

The objective of this work is to present a parameterization of vegetation backscatter effects to be used in the multifrequency, multipolarization application of the IEM in soil moisture retrieval (Bindlish & Barros, 2000; Fung et al., 1992). A short review of existing approaches to model vegetation backscatter is presented next, followed by a description of the proposed parameterization. The utility of the parameterization is tested through the application of SAR data from the Washita 1994 field experiment.

2. Current approaches to modeling backscatter from vegetation canopies

For modeling backscatter from vegetation canopies using radar data, a common approach is to first develop direct models simulating the backscattering coefficient of a canopy with known characteristics. These models can subsequently be used in inverse mode to estimate the characteristics of other canopies. Examples of direct modeling approaches relevant to this work are reviewed next. We group them in three general classes of models: *empirical*, *theoretical*, and *semiempirical*.

2.1. Empirical models

Generally, empirical models have been developed for a single plant structural type (i.e., monospecies plant population) based on the increase of the radar backscattering coefficient (σ^o at frequency band f, polarization p, and incidence angle θ) with biomass according to a power-law relationship in observational data (Ulaby et al., 1986). The backscatter becomes insensitive to increases with biomass at a threshold level (the saturation level), which scales with the wavelength for each species. The HV- and HH-polarized backscatters are found to be the most sensitive to vegetation and hence yield the highest correlations, while the VV-polarized backscatter tends to saturate at lower levels of NDVI. These saturation points define the upper limits for accurate estimation of forest biomass in the case of single frequency and single polarization data (Dobson et al., 1995; Imhoff, 1995). When multifrequency, multipolarization data are available, the range of biomass estimation can be extended beyond that imposed by the "apparent" saturation of a single frequency, single polarization configuration using, for example, polarization ratios (Dobson et al., 1992, 1995; Imhoff, 1995; Pierce, Dobson, Wilcox, & Ulaby, 1993; Ranson & Sun, 1994).

2.2. Theoretical models

In theoretical models of radar scattering, the vegetation canopy is normally treated as a uniform layer of some specified height containing a random distribution of scatterers (Attema & Ulaby, 1978; Eom & Fung, 1984; Fung & Ulaby, 1978; Karam & Fung, 1988; Lang & Sidhu, 1983; Tsang & Kong, 1981). Vegetation can be described as a discrete or as a continuous medium. The discrete model approach for a random layer of vegetation was first used by Du and Peake (1969) to compute the attenuation through a layer of leaves. Later, Karam and Fung (1983), Lang (1981), and Ulaby et al. (1990) have used the approach to develop more rigorous theoretical models for backscatter from a layer of vegetation over the soil surface. The advantage of the discrete approach is that the results are expressed in terms of quantities such as plant geometry and orientation statistics that are easily related to

the biophysical properties of individual plants and can be measured objectively.

Critical limitations in existing theoretical scattering models relate to the assumptions made with regard to the characteristics of the scatterers (Eom & Fung, 1986; Fung, Chen, & Li, 1987; Karam & Fung, 1983, 1988; Lang & Sidhu, 1983; McDonald et al., 1991) or the applicable frequency (Karam & Fung, 1983; Le Vine, Schneider, Lang, & Carter, 1985). Some models account only for leaves but not branches (Eom & Fung, 1986; Fung et al., 1987; Karam & Fung, 1983; Lang & Sidhu, 1983), while others treat branches and the soil surface but not the leaves (Karam & Fung, 1988). In all these models, the scatterers are embedded in one layer above the soil surface or a half-space medium. Ulaby et al. (1990) proposed a two-layer physical model based on the first-order solution of the radiative transfer theory, which was subsequently used by McDonald et al. (1991) to model multiangular and temporal backscatter. Yueh, Kong, Jao, Shin, and LeToan (1992) showed that it is necessary for theoretical models to take into account the architecture of vegetation, which plays an important role in determining the observed coherent effects.

Two major challenges are encountered when modeling the backscatter behavior of a vegetation canopy. The first relates to the difficulties in specifying model parameters that adequately describe the canopy. The second relates to the mathematical complexity in resolving the inverse problem due to the large number of variables and parameters, which makes their inversion difficult (Lang & Sahel, 1985). However, the scattering process involves a certain amount of averaging as a result of the multiple scattering and the quasi-randomness of the locations, sizes, and orientations of the scatterers. This averaging effect, together with specific information about the attenuation properties of a given canopy constituent, makes it possible to make assumptions that simplify the scattering models in terms of physical vegetation parameters. This is the motivation for the semiempirical models.

2.3. Semiempirical models

In order to circumvent these problems, a simpler approach, based on the so-called *water–cloud* model, was developed first by Attema and Ulaby (1978), who proposed to represent the canopy in a radiative transfer model as a uniform cloud whose spherical droplets are held in place structurally by dry matter. The original model was subsequently modified or extended by various authors (Hoekman, Krul, & Attema, 1982; Paris, 1986; Ulaby, Allen, Eger, & Kanemasu, 1984). In water–cloud models, the canopy is represented by "bulk" variables such as leaf-area index (LAI) or total water content, and because of the parsimonious use of parameters, these models can be easily inverted; they are, therefore, good candidates for use in retrieval algorithms (Bouman, 1991). The water–cloud type models are referred to as semiempirical, because model parameters must be derived from (i.e., fitted to) experimental data.

Basic conceptual assumptions in the water–cloud model include: (1) The vegetation is represented as a homogeneous horizontal cloud of identical water spheres, uniformly distributed throughout the space defined by the soil surface and the vegetation height. (2) Multiple scattering between canopy and soil can be neglected. (3) The only significant variables are the height of the canopy layer and the cloud density, the latter assumed to be proportional to the volumetric water content of the canopy. In this context, radar backscattering from a canopy can be expressed as the sum of contributions due to (i) volume scattering in the canopy itself, (ii) surface scattering by the underlying ground surface, and (iii) multiple interactions involving both the canopy and the ground surface. The water–cloud models represent the power backscattered by the whole canopy σ^o as the incoherent sum of the contribution of the vegetation σ^o_{veg} and the contribution of the underlying soil σ^o_{soil}, which is attenuated by the vegetation layer. For a given incidence angle θ, the backscatter coefficient is represented in water–cloud models by the general form:

$$\sigma^o = \sigma^o_{canopy} + \sigma^o_{canopy+soil} + \tau^2\sigma^o_{soil} \quad (1)$$

where τ^2 is the two-way vegetation transmissivity. The first term represents the scattering due to the vegetation canopy, the second term represents the interaction between the vegetation canopy and the soil underneath and accounts for multiple scattering effects, and the third term represents the scattering from the soil layer. The vegetation–soil interactions are neglected in the water–cloud model, and, therefore,

$$\sigma^o = \sigma^o_{veg} + \tau^2\sigma^o_{soil} \quad (2)$$

with

$$\tau^2 = \exp(-2Bm_v\sec\theta) \quad (3)$$

and

$$\sigma^o_{veg} = Am_v\cos\theta(1-\tau^2) \quad (4)$$

where m_v is the vegetation water content (kg/m^2). A and B are parameters depending on the canopy type. The constant A is the maximum allowable attenuation from the vegetation canopy (both $\cos\theta$ and $[1-\tau^2]$ are less than 1). Thus, A can be interpreted as a vegetation density parameter (0 for bare soil, a very high value for evergreen forests). This formulation corresponds to the first-order solution of radiative transfer equation through a weak medium, where multiple scattering effects can be neglected.

The variations in the canopy descriptors used in the models that describe canopy backscattering are due to the complexity of vegetation structure and to the relative simplicity of the models: There is no general theoretical basis to define the best set of canopy descriptors, and consequently, to derive the values of the A and B parameters. Furthermore, for a given canopy, strong functional relationships exist

between these canopy descriptors. As a matter of fact, the geometrical structure of the canopy is implicitly accounted for through these parameters A and B, which are always determined by fitting the models against experimental data sets. The maximum backscatter attenuation reported in the literature is about 3 dB (deciduous forests, Ulaby et al., 1986). One would expect vegetation attenuation from tropical rain forests and dense evergreen forests to be higher, and, thus, the applicability of the water–cloud model for such applications requires further evaluation.

In order to account for possible heterogeneity of canopies due to the existence of vertical variations or different types of scatterers (leaves, stems, etc.), multilayer or multicomponent water–cloud models were also developed, yet, without significant improvement in the results (Bernard, Frezal, Vidal-Madjar, Guyon, & Riom, 1987; Hoekman et al., 1982; Ulaby et al., 1984).

One approach that has provided encouraging results is the use of multifrequency data in the water–cloud model. This approach is based on the premise that such data and combinations thereof are sensitive to different components of the vegetation canopy. Various authors including Bouman (1991), Hoekman et al. (1982), and Ulaby et al. (1984) stressed, however, the strong sensitivity of the parameters in the water–cloud models to small changes in land-cover. This restricts the generalized use of the approach, because the sensitivity of the parameters to changes in canopy structure will also affect the robustness of the inversion scheme.

Although it is almost certainly impossible to define a universal semiempirical inversion algorithm, in principle, it should be possible to develop one for each class of vegetation as defined by geometric structure. This was the motivation for this study, and a parameterization of vegetation backscatter is proposed next, which attempts to account for effects of geometric structure and spatial variability.

3. Vegetation backscattering parameterization

The backscattering coefficient of the canopy is interpreted here in the framework of semiempirical water–cloud models: (1) Both the canopy loss and the vegetation volume scattering coefficient are linked to the canopy's biophysical properties, and especially, but not exclusively, to canopy type, canopy structure, and the water volume fraction within the canopy. (2) The canopy loss and the volume scattering coefficient increase with frequency. (3) The vegetation term tends to dominate the net return as either frequency or incidence angle increases. (4) The interactive term functions to enhance radar sensitivity to the moisture contained in the soil beneath a vegetation canopy.

In the classic water–cloud model, the backscattering in the presence of vegetation is approximated as a combination of the individual backscatter from the vegetation canopy and the underlying soil layer as given by Eq. (2). As mentioned previously, the orientation and geometry of the vegetation are key governing factors for vegetation backscatter. Furthermore, it is possible that two or more tree canopies overlap and are caught in the same radar beam. Layover occurs when one or more canopies of different heights are located at the same range distance, and the vegetation backscatter from one is affected by the other and vice versa. In this case, the standard water–cloud model will account for scattering of the same beam by two different trees, which could lead to overestimating the vegetation backscatter where canopy layover occurs. This effect is referred hereafter as radar-shadow effect.

3.1. Radar-shadow effect

As reviewed earlier, the linear dependence of σ^o (Eq. (1)) on forest biomass has been found to decrease with frequency as scattering and attenuation by the crown layer of foliage and small branches become more significant. In particular, the polarizations most sensitive to specular scattering mechanisms by the trunk and ground surface (HH and HV) show the highest sensitivity to biomass, whereas the linear dependence of σ^o on biomass tends to saturate at biomass levels which scale with wavelength (Dobson et al., 1992). Sun and Ranson (1995) showed that cross-polarization signatures are more sensitive to the crown structure than the like-polarization signatures. Specifically, the ratio of HV backscattering from a longer wavelength (P or L) to that from a shorter wavelength (C) appears to be a good combination for mapping forest biomass. This ratio enhances the correlation of the image signature with the standing biomass, and compensates for part of the variations in backscattering attributed to radar incidence angle (Sun & Ranson, 1995).

The relationship between backscatter and biomass is investigated next using the Washita 1994 data for the Little Washita watershed in southwest Oklahoma. During the experiment, the land was covered by rangeland, pasture, winter wheat, corn, and alfalfa. A complete description of the watershed is available in Allen and Naney (1991) or Starks and Humes (1996). The radar data consist of 6 days of SIR-C/X-SAR data in three different bands and different polarizations: L-band (23.5 cm), C-band (5.8 cm), and X-band (3.1 cm). NDVI was used as a quantitative proxy of biomass. Table 1, which is replicated from Bindlish and Barros (2000), provides a description of the data collected during Washita 1994. Further details can be found in Jackson et al. (1996). Table 2 shows the values of correlation coefficients between backscatter and NDVI for different frequencies and polarizations, and for different land-use classes, using both linear and exponential approximations. Note that the correlation coefficient increases to 0.5 (maximum value of 1.6) from around 0.3 (maximum value of 0.4), when an exponential function is used instead of a linear relationship. As expected, there is also a substantial difference between the values obtained when cross-polarizations are used.

According to these empirical results, we propose an exponential vegetation correlation function to model the

effect of "radar shadow," or vegetation layover. The geometric effect of vegetation spacing can be accounted for by introducing the concept of dimensionless vegetation correlation length, which is a function of the distance at which the plants function as independent scatterers. The vegetation correlation length can be interpreted as a bulk measure of the effects of the shape, size, and spatial distribution of individual plant canopies. Hence, it varies with plant type, stage of growth, and in general, with the 3D architectural layout of vegetation in the landscape. Formally, the effect of vegetation layover is described as follows:

$$\sigma^{o^*}_{veg} = \sigma^{o}_{veg}[1 - \exp(-\alpha)] \quad (5)$$

where σ^{o*}_{veg} is the corrected vegetation contribution, and α is the radar-shadow coefficient ($\alpha \geq 0$). The radar-shadow coefficient (or dimensionless vegetation correlation length $\alpha = L_{veg}/L$) should vary with vegetation type and with land-use and/or the spatial variability of land-cover in the landscape. The dimensionless vegetation correlation length used here is conceptually similar to the surface correlation length for soils used in the IEM (Fung et al., 1992). The characteristic length scale L is the field scale at which representative ground measurements are available. Accordingly, Eq. (2) must be modified to reflect the explicit representation of the radar-shadow effect:

$$\sigma^{o} = \sigma^{o^*}_{veg} + \tau^2 \sigma^{o}_{soil} \quad (6)$$

3.2. Parameter estimation

To estimate the three vegetation parameters A, B, and α, the IEM model (Fung et al., 1992) is used first in the forward mode to calculate "bare-soil" backscatter coefficients σ^{o}_{soil} at locations where ground-based measurements of soil moisture and other ancillary data are available. The ratio between the measured backscatter coefficients σ^{o} and σ^{o}_{soil} is the vegetation transmissivity τ^2. Subsequently, the value of B can be calculated directly from Eq. (3), and σ^{o}_{veg} can be obtained from Eq. (2). The parameters A and α are obtained from Eqs. (5) and (6), where σ^{o}_{veg} is replaced by the right-hand side of Eq. (4). When data exist at multiple sites, Least Mean Squares (LMS) regression analysis is necessary to include data from all locations.

In principle, if multifrequency data are available, different values of A, B, and α can be derived for each frequency. For the application presented here, we calculate independently of the frequency, only one set of parameters for each vegetation category. The relative weight of different frequencies in the regression analysis is determined according to Ulaby et al. (1986), who showed that the combined effects of volume scattering in the water–cloud model and the geometric scattering vary approximately as f^2, which is (Eq. (7)):

$$\sigma^{o^*}_{veg} \propto f^2 \quad (7)$$

One of the advantages of this approach is that all the vegetation parameters (A, B, and α) can be defined using ancillary data. Thus, it should be possible to use this parameterization for operational soil moisture monitoring.

Table 1
Daily specification of the SIR-C/X-SAR data for Washita 1994

Day (April 1994)	Flight direction	Incidence angle (°)	Bands and polarizations
11	A	28.0	L_{HH}, L_{VV}, L_{HV}, C_{HH}, C_{VV}, C_{HV}, X_{VV}
12	A	42.3	L_{HH}, L_{VV}, L_{HV}, C_{HH}, C_{VV}, C_{HV}, X_{VV}
13	A	50.1	L_{HH}, L_{VV}, L_{HV}, C_{HH}, C_{VV}, C_{HV}, X_{VV}
14	A	56.3	L_{HH}, L_{HV}, C_{HH}, C_{HV}, X_{VV}
14	D	48.3	L_{HH}, L_{HV}, C_{HH}, C_{HV}, X_{VV}
15	A	60.2	L_{HH}, L_{VV}, L_{HV}, C_{HH}, C_{VV}, C_{HV}
15	D	42.4	L_{HH}, L_{VV}, L_{HV}, C_{HH}, C_{VV}, C_{HV}, X_{VV}
16	D	36.2	L_{HH}, L_{VV}, L_{HV}, C_{HH}, C_{VV}, C_{HV}, X_{VV}
17	D	30.9	L_{HH}, L_{VV}, L_{HV}, C_{HH}, C_{VV}, C_{HV}
18	D	26.5	L_{HH}, L_{VV}, L_{HV}, C_{HH}, C_{VV}, C_{HV}, X_{VV}

A = ascending pass; D = descending pass.

Table 2
Regression constants for linear and exponential fits to the empirical relationship between backscatter coefficient and NDVI for the Washita 1994 study area

Frequency and polarization	Rangeland		Winter wheat		Pasture	
	Linear	Exponential	Linear	Exponential	Linear	Exponential
C_{HH}	0.23	0.45	0.26	0.48	0.24	0.40
C_{HV}	0.26	0.48	0.28	0.52	0.25	0.42
L_{HV}	0.21	0.41	0.22	0.46	0.19	0.32
L_{HH}	0.25	0.56	0.25	0.51	0.22	0.39
L_{VV}	0.18	0.38	0.20	0.42	0.23	0.41
C_{HH}/L_{HH}	0.30	0.56	0.32	0.58	0.28	0.53
C_{HH}/L_{HV}	0.33	0.58	0.36	0.61	0.28	0.52
C_{HV}/L_{HV}	0.33	0.59	0.34	0.55	0.31	0.56
C_{HV}/L_{HH}	0.29	0.55	0.36	0.62	0.29	0.50

4. Application

The multifrequency, multipolarization inversion model based on the IEM used by Bindlish and Barros (2000) was modified by introducing the vegetation backscatter parameterization proposed above, and the Washita 1994 soil moisture inversion application described therein was repeated.

4.1. Specification of vegetation parameters

First, the IEM was run in the forward mode to estimate the independent backscatter contribution from the soil (see

Table 3
Site characterization for Washita 1994 April mission

Site	Vegetation water content (g/m^2)	Surface roughness (cm)	Land cover
11	1798	0.81	Alfalfa
12	0	3.43	Bare soil
13	1386	0.81	Winter wheat
14	96	0.73	Rangeland
21	78	0.87	Rangeland
22	107	0.67	Rangeland
23	65	1.31	Rangeland
31	797	0.99	Winter wheat
32	1933	0.56	Winter wheat
33	1916	0.85	Winter wheat
34	103	0.49	Pasture
53	797	1.18	Winter wheat
54	86	0.76	Pasture
55	817	0.73	Winter wheat
71	0	0.55	Bare soil

right-hand side of Eq. (2)) at each site where gravimetric soil moisture experiments were conducted during Washita 1994 (15 sites in all, Table 3). The vegetation parameters A, B, and α were subsequently derived as described above. Table 4 shows the values of the vegetation constants when all land used are lumped together and separately for the sites where both ground-based measurements of soil moisture and vegetation were available. Three different land-use classes (rangeland, winter wheat, and pasture) fell in the latter category (12 of the 15 sampling sites in Table 3). Finally, the full inversion model was run to estimate the soil moisture fields for all 6 days during Washita 1994. Two different experiments were conducted: In the first case, the vegetation parameters were specified without taking into consideration the land-use class of each pixel, and, thus, only one value of each parameter is used for the entire area (first column in Table 4). In the second case, the land-use specific parameters were used whenever the pixel fell in one of the three categories (winter wheat, pasture, and rangeland), and the average values were used elsewhere.

In the first experiment, the use of the explicit parameterization of vegetation backscatter in the soil moisture inversion resulted in a small increase ($\approx$5%) in the correlation coefficient between retrieved and measured soil moisture: R=.87 as compared to R=.83, obtained by Bindlish and Barros (2000), when no vegetation correction was used. Fig. 1 shows the scatter plot of measured vs. retrieved soil moisture with and without using the explicit vegetation parameterization, with only one set of parameters (A, B, α) identical for all vegetation and land-use types.

Table 4
Values of vegetation parameters used in the semiempirical model

	All land-uses	Rangeland	Winter wheat	Pasture
A	0.0012	0.0009	0.0018	0.0014
B	0.091	0.032	0.138	0.084
α	2.12	1.87	10.6	1.29

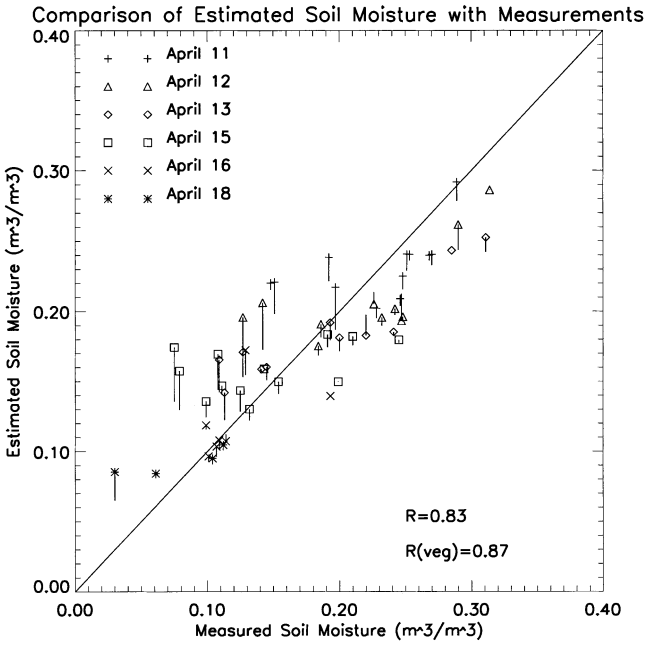

Fig. 1. Scatter plot of measured volumetric soil moisture and estimated volumetric soil moisture for all the sampling sites for the entire duration of the Washita 1994 experiment using the vegetation parameterization with the same set of parameters (A, B, α) for all land-use types (first column in Table 4).

The use of common vegetation parameters for the entire study area does not allow the model to differentiate between various vegetation canopies, and, thus, the geometric effect of canopy structure and spatial layout of individual canopies (here assumed to be a function of land-use) was not accounted for. However, in the second experiment, the correlation coefficient improved up to 0.95 (see Fig. 2), which corresponds to a decrease of about 32% in the average RMSE for this application. That is, by introducing land-use class in the determination of the vegetation parameters, a substantial skill improvement was achieved in describing the specific structural features of vegetation associated with dampening of surface backscatter.

Note that, for this case-study, the maximum vegetation amount anywhere in the watershed was moderate (less than 2 kg/m^2, Table 3). None of the sampling sites had dense vegetation, which is true for most of the watershed. The saturation levels reported by Imhoff (1995) were as follows: C-band $\approx$ 2 kg/m^2, L-band $\approx$ 4 kg/m^2, and P-band $\approx$ 10 kg/m^2. Thus, none of the sampling sites was above the saturation level for C-band, and all sites were well below the L-band saturation levels. This could be one of the reasons for the success of this parameterization. The current model must, therefore, be tested under more diverse conditions in order to perform a compre-

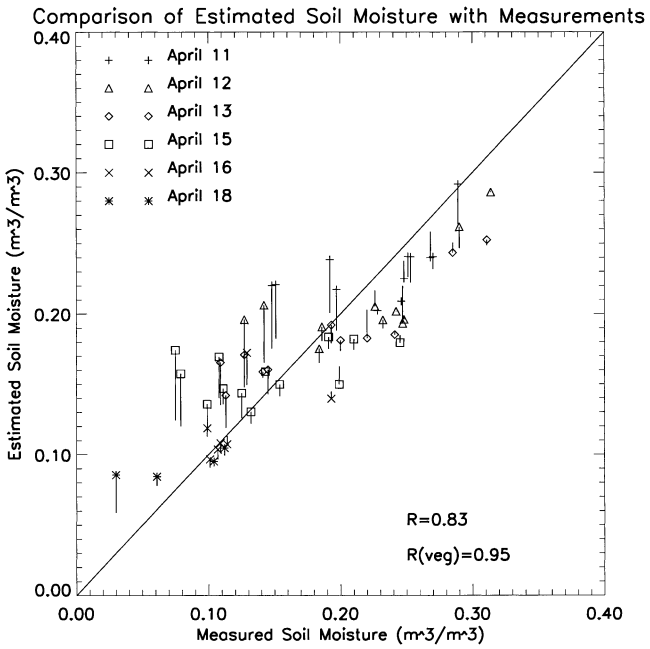

Fig. 2. Scatter plot of measured volumetric soil moisture and estimated volumetric soil moisture for all the sampling sites for the entire duration of the Washita 1994 experiment using the vegetation parameterization with different sets of parameters (A, B, α) for different land-use types (Table 4).

hensive evaluation of its effective skill to "see through" dense vegetation.

In principle, the land-use-class-based approach requires separate empirical relationships for each vegetation type, and, thus, the need to carry out large-scale vegetation characterization studies such as those conducted for field experiments like Washita 1994. Long-term field measurements of vegetation parameters at pilot sites are needed, since these parameters will change with both natural and anthropogenic vegetation changes. However, given that reliable land-use/land-cover maps are available (or can be generated from remotely sensed imagery in the visible portion of the spectrum) at timescales consistent with local vegetation changes, the parameter specification problem can be resolved with an adaptive algorithm to adjust the parameters as dictated by sequential changes in the remotely sensed multifrequency radar data.

5. Summary

The objective of this work was to formulate and test an explicit parameterization of vegetation backscatter effects in the retrieval of soil moisture from radar data. The solution proposed was patterned after the water–cloud model and modified by introducing a semiempirical parameterization to account for radar-shadow effects. The use of this explicit vegetation parameterization in a multifrequency, radar-based, soil moisture retrieval model improved significantly the soil moisture retrieval for vegetated pixels during Washita 1994.

Two different experiments were conducted for coupling the water–cloud model with the multifrequency, radar-based, soil moisture estimation algorithm. In the first approach, the effect of vegetation-specific structure was neglected, and the results obtained were only marginally better than those reported by Bindlish and Barros (2000). However, the results were significantly better when land-use class was introduced explicitly in the specification of vegetation parameters. This is consistent with the notion that vegetation density and water content are not sufficient to represent vegetation backscattering effects, and, therefore, some measure of the spatial variability and architectural layout of vegetation is required (see, for example, Yueh et al., 1992). Thus, the dimensionless vegetation correlation length can be viewed as a first-order bulk measure of the geometric backscatter effects of the prevailing characteristic spatial scales of land-use/land-cover classes in the landscape (e.g., compare α for winter wheat with that for pasture and rangeland in Table 4). Although encouraging, this proposition and the utility of the vegetation correlation length concept must be further investigated in forests and densely vegetated areas, and in environments and climatic regions where the spatial and temporal variability of vegetation are markedly strong.

Acknowledgments

This research was funded by NASA under contracts NAGW-5254 and NAGW-2686 with the second author through the Earth System Science Center at Penn State University.

References

Allen, P. B., & Naney, J. W. (1991). *Hydrology of the Little Washita River Watershed, Oklahoma: data and analysis* (USDA/ARS-90, 74 pp.).

Asrar, G., Kanemasu, E., Jackson, R., & Pinter, P. (1985). Estimation of total above ground phytomass production using remotely sensed data. *Remote Sensing of Environment*, *23*, 577–587.

Attema, E. P. W., & Ulaby, F. T. (1978). Vegetation modeled as a water cloud. *Radio Science*, *13*, 357–364.

Bernard, R., Frezal, M., Vidal-Madjar, D., Guyon, D., & Riom, J. (1987). Nadir looking airborne radar and possible applications to forestry. *Remote Sensing of Environment*, *21*, 297–309.

Bindlish, R., & Barros, A. P. (2000). Multi-frequency soil moisture inversion from SAR measurements using IEM. *Remote Sensing of Environment*, *71* (1), 67–88.

Bouman, B. (1991). Crop parameter estimation from ground based X-band (3 cm wave) radar backscattering data. *Remote Sensing of Environment*, *37*, 193–205.

Cimino, J., Casey, A. D., Rabassa, J., & Wall, S. D. (1986). Multiple incidence angle SIR-B experiment over Argentina: mapping of forest units. *IEEE Transactions on Geosciences and Remote Sensing*, *24*, 498–509.

Dobson, M. C., Ulaby, F. T., Le Toan, T., Beaudoin, A., Kasischke, E. S., &

LeToan, T. (1992). Dependence of radar backscatter on coniferous forest biomass. *IEEE Transactions on Geosciences and Remote Sensing*, *21*, 44–55.

Dobson, M. C., Ulaby, F. T., Pierce, L. E., Sharik, T. L., Bergen, K. M., Kellndorfer, J., Kendra, J. R., Li, E., Lin, Y. C., Nashashibi, A., Sarabandi, K., & Siqueira, P. (1995). Estimation of forest biophysical characteristics in northern Michigan with SIR-C/X-SAR. *IEEE Transactions on Geosciences and Remote Sensing*, *33*, 877–895.

Du, L., & Peake, W. H. (1969). Rayleigh scattering from leaves. *Proceedings of IEEE Geosciences and Remote Sensing Symposium*, *57*, 1227–1229.

Eom, H. J., & Fung, A. K. (1984). A scatter model for vegetation up to Ku-band. *Remote Sensing of Environment*, *19*, 139–149.

Eom, H. J., & Fung, A. K. (1986). Scattering from a random layer embedded with dielectric needles. *Remote Sensing of Environment*, *15*, 185–200.

Fung, A. K. (1994). *Microwave scattering and emission models and their application*. Boston: Artech House.

Fung, A. K., Chen, M. F., & Li, K. K. (1987). Fresnel field interaction applied to scattering from a vegetation layer. *Remote Sensing of Environment*, *23*, 35–50.

Fung, A. K., Li, Z., & Chen, K. S. (1992). Backscattering from a randomly rough dielectric surface. *IEEE Transactions on Geosciences and Remote Sensing*, *30* (2), 356–369.

Fung, A. K., & Ulaby, F. T. (1978). A scatter model for leafy vegetation. *IEEE Transactions on Geosciences and Remote Sensing*, *16*, 281–286.

Hoekman, D., Krul, L., & Attema, E. (1982). A multi-layer model for radar backscattering by vegetation canopies. *IEEE–IGARSS '82*, *2*.

Imhoff, M. L. (1995). Radar backscatter and biomass saturation: ramifications for global biomass inventory. *IEEE Transactions on Geosciences and Remote Sensing*, *33* (2), 511–518.

Jackson, T. J., Tang, L., Hsu, A., Wood, E., O'Neill, P. E., & Engman, E. T. (1996). *Washita '94 SIR-C/X-SAR datasets*. Greenbelt, MD: NASA Goddard Space Flight Center (Published on CD-ROM).

Karam, M. A., & Fung, A. K. (1983). Scattering from randomly oriented circular disc with application to vegetation. *Radio Science*, *18*, 557–565.

Karam, M. A., & Fung, A. K. (1988). Electromagnetic scattering from a layer of finite length, randomly oriented, dielectric circular cylinders over a rough interface with application to vegetation. *International Journal of Remote Sensing*, *9*, 1109–1134.

Lang, R. H. (1981). Electromagnetic backscattering from a random distribution of lossy dielectric scatterers. *Radio Science*, *16*, 15–30.

Lang, R. H., & Sahel, H. (1985). Microwave inversion of leaf area index and inclination angle distributions from backscattered data. *IEEE Transactions on Geosciences and Remote Sensing*, *23*, 685–694.

Lang, R. H., & Sidhu, J. S. (1983). Electromagnetic backscattering from a layer of vegetation: a discrete approach. *IEEE Transactions on Geosciences and Remote Sensing*, *21*, 62–71.

Le Vine, D. M., Schneider, A., Lang, R. H., & Carter, H. G. (1985). Scattering from thin dielectric disks. *IEEE Transactions on Antennas and Propagation*, *33*, 1410–1413.

McDonald, K. C., Dobson, M. C., & Ulaby, F. T. (1991). Modeling multifrequency diurnal backscatter from a walnut orchard. *IEEE Transactions on Geosciences and Remote Sensing*, *29*, 852–863.

Paris, J. (1986). The effect of leaf size on the microwave backscattering by corn. *Remote Sensing of Environment*, *19*, 81–95.

Pierce, L. E., Dobson, M. C., Wilcox, E., & Ulaby, F. T. (1993). Artificial neural network inversion of tree canopy parameters in the presence of diversity. *Proceedings of IGARSS '93*, 394–397.

Prevot, L., Dechmbre, M., Taconet, O., Vidal-Madjar, D., Normand, M., & Galle, S. (1993). Estimating the characteristics of vegetation canopies with airborne radar measurements. *International Journal of Remote Sensing*, *14*, 2803–2818.

Ranson, K. J., & Sun, G. (1994). Mapping biomass of a northern forest using multifrequency SAR data. *IEEE Transactions on Geosciences and Remote Sensing*, *32*, 388–396.

Sellers, P. (1985). Canopy reflectance, photosynthesis and transpiration. *International Journal of Remote Sensing*, *6*, 1335–1375.

Starks, P. J., & Humes, K. S. (1996). *Hydrology data report Washita '94,* USDA NAWQL 96-1.

Sun, G., & Ranson, K. J. (1995). A three-dimensional radar backscattering model of forest canopies. *IEEE Transactions on Geosciences and Remote Sensing*, *33* (2), 372–382.

Taconet, O., Benallegue, M., Vidal-Madjar, D., Pervot, L., Dechambre, M., & Normand, M. (1994). Estimation of soil and crop parameters for wheat from airborne radar backscattering data in C and X bands. *Remote Sensing of Environment*, *50*, 287–299.

Tsang, L., & Kong, J. (1981). Application of strong fluctuation random medium theory to scattering from vegetation-like half space. *IEEE Transactions on Geosciences and Remote Sensing*, *19*, 62–69.

Tucker, C., Vanpraet, C., Sharman, M., & Van Ittersum, G. (1985). Satellite remote sensing of total herbaceous biomass production in the Senegalese Sahel. *Remote Sensing of Environment*, *17*, 233–249.

Ulaby, F. T., Allen, C. T., Eger, G., & Kanemasu, E. (1984). Relating microwave backscattering coefficient to leaf area index. *Remote Sensing of Environment*, *14*, 113–133.

Ulaby, F. T., Moore, R. K., & Fung, A. K. (1986). *Microwave remote sensing: active and passive, vols. 1–3*. Dedham, MA: Artech House.

Ulaby, F. T., Sarabandi, K., McDonald, K., Whitt, M., & Dobson, M. C. (1990). Michigan microwave canopy scattering model. *International Journal of Remote Sensing*, *11*, 1223–1253.

Wu, S. T. (1987). Potential application of multi-polarization SAR for plantation pine biomass estimation. *IEEE Transactions on Geosciences and Remote Sensing*, *25*, 403–409.

Yueh, S. H., Kong, J. A., Jao, J. K., Shin, R. T., & LeToan, T. (1992). Branching model for vegetation. *IEEE Transactions on Geosciences and Remote Sensing*, *30*, 390–402.